

Mohamed F. Yassin^{a,*}, Masaaki Ohba^b, Hideyuki Tanaka^b^aFaculty of Engineering, Assiut University, Assiut, Egypt^bDept. of Architecture Engineering, Tokyo Polytechnic University, Atsugi, Japan**ABSTRACT**

To assist validation of numerical models of urban pollution dispersion, the effect of obstacles on the flow and pollutant dispersion have been investigated experimentally in the boundary layer wind tunnel under neutral atmospheric conditions using a tracer gas technique from a point source without buoyancy. The flow and diffusion fields in the boundary layer in an urban environment were investigated in the downwind distance of the obstacle model using an isolated high-rise building model. The scale of the model experiment was assumed to be at 1:1000. In the experiment, gaseous pollutant was discharged in the simulated boundary layer over the flat terrain. The effluent velocity of the pollutant was set to be negligible. The velocity field and the turbulence characteristics were analyzed and measured using a hot wire anemometer with a split-fibre probe. The experimental technique was involved the continuous release of tracer gas from a ground level source which was located in the downwind distance of the obstacle model and measured using a fast flame ionization detector (FID). Diffusion characteristics were studied and included both the vertical and lateral mean concentrations and concentration fluctuation intensity at various downwind distances. The results of study were demonstrated that the vertical profiles of the longitudinal mean velocity are very thick around the obstacle wake region due to the turbulence mixing and the smoothing of concentration differences was increased with downwind distance from the obstacle model. Furthermore, the experimental results can help to improve the understanding of mechanisms of pollutant dispersion in an urban environment and also use to validate the corresponding computational fluid dynamics (CFD) prediction.

Keywords: Air flow; Concentration fluctuation; Dispersion; Obstacles model; Wind tunnel

1. INTRODUCTION

The study of the effect of obstacles on flow and dispersion in the atmospheric boundary layer is one of the most important topics of air pollution research. Therefore, increasing concern over the problem of atmospheric pollution in an urban environment has highlighted the need for detailed investigations of atmospheric flow and dispersion of contaminants in the vicinity of buildings. Experimental investigation on flow and dispersion around an isolated obstacle is very useful in identifying the effect of a building or any other construction on the behavior of effluents plumes released in their vicinity. Moreover, information of the flow characteristics near an isolated obstacle may be used to describe the region close to

a discharge in the development of an urban dispersion model.

In recent years, a significant amount of work has been concentrated to studying the effect on the problem of flow around isolated obstacle and to a lesser extent on small groups of obstacles on atmospheric dispersion. Both wind tunnel and field experiments have shown that strong effects can be introduced by the wake flow near the obstacle and that wind tunnel experiments can provide a good basis for predicting wake dispersion in the real atmosphere. However, a little discussion of concentration variability, particularly that in rather complicated flow immediately in the lee of an obstacle has been published. Hunt and Mulhearn (1973) have developed the application of complex models of dispersion around two dimensional obstacles. Meroney (1982) provided an extended review of the main characteristics of flow and dispersion near building. Castro and Snyder (1982) and others have reported the study of the

**Corresponding author address:*

Mohamed F. Yassin, (*Visiting researcher*),
Dept. of Architecture Engineering, Tokyo Polytechnic
University, 1583 Iiyama, Atsugi, Kanagawa, Japan
E-mail: mfy_64@yahoo.com / mfy@aun.edu.eg

flow and dispersion around a single surface mounted obstacle in a boundary layer wind tunnel. Recently, Kim et al. (1990) and Higson et al. (1994) have investigated flow and dispersion around individual or small groups of obstacles. Davidson et al. (1995, 1996) investigated the flow and dispersion through large group's obstacles, both in field and wind tunnel experiments. MacDonald et al. (1997, 1998) have described the effect of obstacle aspect ratio on dispersion in obstacle arrays in field and wind tunnel experiments. Dispersion of atmospheric pollutants in the vicinity of isolated obstacles of different shape and orientation with respect to the mean wind direction (Mavroidis et al. 1999, 2001, 2003 and others) have been examined in scaled field and wind tunnel experiments.

This paper presents the results of an experimental investigating for studying the effect of isolated obstacle on the flow and pollutant dispersion in the boundary layer in an urban environment using a tracer gas without buoyancy under neutral atmospheric conditions at various locations in the downwind distance of the obstacle model using an isolated high-raise building model. Therefore, the aim of the present work is to improve the understanding of mechanism of pollutant dispersion with effect of obstacles in an urban environment and also use to validate the corresponding computational fluid dynamics (CFD) prediction. In the study of the concentration behavior, the general non-dimensional concentration K was used as the ratio of the mean concentration C at any point in the wind tunnel experiments to a reference concentration C_o :

$$K = C / C_o \quad (1)$$

$$C_o = \frac{q}{U_H H^2} \quad (2)$$

Where, H is the reference height, U_H is the reference velocity, and q is the contaminant release rate.

2. EXPERIMENTAL FACILITIES AND MEASUREMENTS

2.1. Wind tunnel facility

The facility used was the wind tunnel at the Tokyo Polytechnic University, Japan. The wind tunnel was designed specially to model atmospheric boundary layer. The tunnel is of open

circuit facility. The width and height of the test tunnel are 1.2 m and 1 m respectively. The upwind fetch is 14 m. A turbulent boundary layer for the neutral atmospheric conditions in an urban environmental was simulated on a scale of 1:1000. The obstacles used in the flow and diffusion fields was isolated high rise building model with height 200mm, width 100 mm and length 100m. The power law $U \propto Z^n$ was applied to the vertical wind profile. The typical value of $\frac{1}{4}$ for the power number n in an urban area was employed. However there is a range of other possible values for n . For details of such typical values of the power law exponent for different terrain types, refer to Snyder (1981).

2.2. Velocity and Turbulence measurements

The flow structure was measured using hot-wire anemometry with split fibre probe, which was 55R55 straight probe, had sensors perpendicular to the probe axis and was set to have the plane of split normal to the free stream. Thus, it was able to detect reversals of the local flow direction. The split fiber probe was oriented to measure longitudinal and vertical components (u and w) and longitudinal and lateral components (u and v) of velocity starting at 7 mm above the floor of the wind tunnel. Split fiber probes have been used for investigating the structure of a turbulent separation bubble as reported by Kiya and Sasaki (1983). The calibration procedures of split fiber probes for air flow have been described by Boerner and Leutheusser (1984) and others. The rotation speed of the wind tunnel fan was kept constant during the experiment to achieve a steady free stream velocity of about 1.3 ms⁻¹. This was monitored with a Pitot-tube and a single hot-wire. Both were positioned at the wind tunnel centerline, 50 cm above the floor, a few centimeters upstream of the leading edge of the upstream urban fetch. During measurements, the signals from the Pitot-tube and hot-wire were digitally recorded for 60 s on a desktop PC.

2.3. Concentration Measurements

Dispersion experiments were undertaken by releasing gas at a controlled rate from the point source, sampling the air downwind and then analyze the samples to obtain the concentration of emitted gas that they contain. The source flow rate was controlled by Vol-U-Meter Automatic Gas Flow. The tracer gas chosen, in this case is ethylene, C_2H_4 , which was emitted from the point source at $X/H = 0.125$ that has an inner diameter

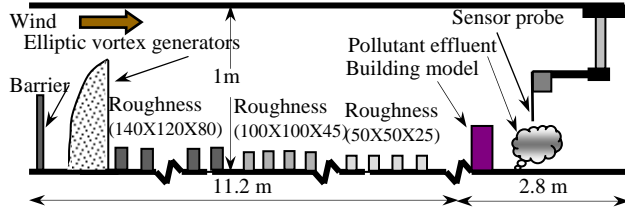


Fig. 1. Schematic diagram of the wind tunnel experiments

of 4 mm. High response flame ionization detector (FID) was used to measure the C_2H_4 concentration. The concentrations were obtained by collecting samples through the pipeline attached to the carriage system in the tunnel. The samples were routed to the FID which produced output voltages linearly related to concentration. The output voltage from the FID was sampled by minicomputer system at a rate of 1 Hz over averaging time of 60 s, which was sufficient to obtain stable values of the fluctuation concentration. The fluctuation concentration and wind speed were measured simultaneously together at the same time in this experiment. In the present study, the emission velocity from the point source is smaller than that of free stream velocity. Therefore, the effluent velocity of the pollutant is assumed to be negligible. Since a density of C_2H_4 gas is almost same with that of air, the density of pollutant gas can be thought to have the same density at the height of the pollutant effluent in the boundary layer.

3. RESULTS AND DISCUSSIONS

3.1 Simulated boundary layer

A simulated atmospheric boundary layer was obtained by using a combination of barrier wall, elliptic vortex generators and roughness elements on the floor of the tunnel as shown in the schematic diagram of Fig.1. This combination of barriers, vortex generators and roughness elements produced a simulated atmospheric boundary layer with a normal depth, δ , of 0.6 m and a free stream wind speed, U_∞ of 1.3 ms^{-1} .

The resulting Reynolds number, R_e

$$R_e = \frac{U_\infty \delta}{\nu} \quad (3)$$

where; U_∞ = free steam velocity, δ = boundary layer thickness and ν = kinematics viscosity. In the approaching flow, R_e was approximately 5.2

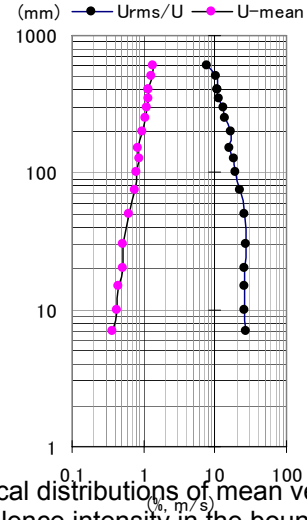


Fig. 2. Vertical distributions of mean velocity and turbulence intensity in the boundary layer.

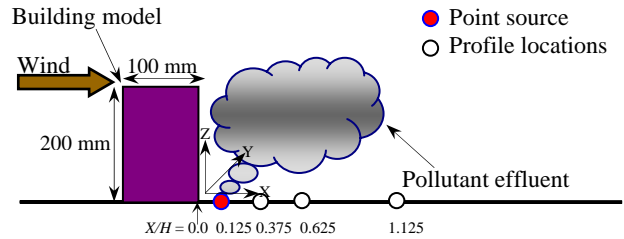


Fig. 3. Building model, point source and profile locations in wind tunnel

$\times 10^4$, which is above the threshold (4×10^3) for Reynolds number independence of dynamic similarity for flow around of cube model (Mfula et al, 2005).

Fig. 2 shows the simulated turbulent boundary layer in the atmospheric boundary layer wind tunnel under neutral atmospheric conditions at $x = 0.0$ (the center of turntable). All wind profiles show almost linear profiles in the vertical direction.

3.2. The influence of obstacle on the flow characteristics

The flow characteristics measurements were made at four different spots along the centerline of the wind tunnel; $X/H = 0.125, 0.375, 0.625$ and 1.125 , which is shown in Fig. 3. The flow obstacle model was located at $X/H = 0.0$. The vertical profiles of mean flow were measured in the turbulent boundary layer starting at 7 mm above the ground level of the wind tunnel under neutral atmospheric conditions. The mean velocity components are normalized by the mean velocity U_h obtained, which is the approaching wind velocity at the building height H in the boundary layer.

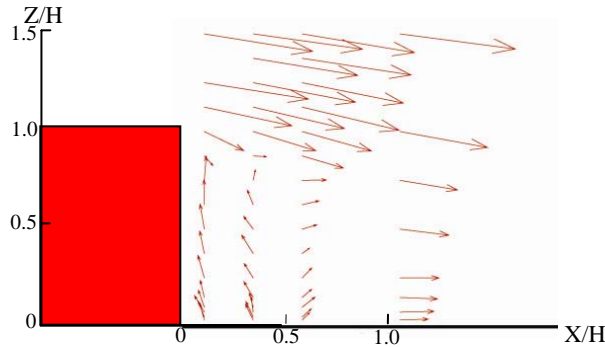


Fig. 4. Mean velocity vectors around the obstacle wake

3.1.1 Mean velocity vectors

The mean velocity vectors around the obstacle wake region are shown in Fig. 4. Inverse flows were observed clearly up to a height of $Z/H = 0.625$ in the obstacle wake region; $X/H = 0.125$ and 0.375 .

3.1.2 Mean velocity

The vertical profiles of mean velocity in the longitudinal, lateral and vertical components (u , v , w) are shown in Figs. 5 to 7. The longitudinal mean velocity U was increased up near the obstacle top and decreased down to the ground surface. The vertical profiles of the longitudinal mean velocity U were appeared very thick around the obstacle wake region at $X/H = 0.125$, 0.375 and 0.625 . This is due to the large effect of turbulent mixing, which is created by the distortion of flow in the wake region. Therefore, this makes small separation at this region. While, a thin vertical profile was generated at $X/H = 1.125$.

The vertical wind velocity W was directed upward and reaches a minimum value near the obstacle top at $X/H = 0.125$, 0.375 , and 0.625 , while, a maximum value was observed near the ground level at $X/H = 0.125$, 0.375 and 0.625 due to the steep gradient of the vertical turbulence intensity. The change of the lateral mean velocity V distribution at $X/H = 0.125$, 0.375 , 0.625 and 1.125 are much going downwind distance starting near the obstacle top to the ground level. This is due to the higher lateral turbulence intensity.

3.1.3 Turbulence intensity

The vertical profiles of turbulence intensity in the longitudinal, lateral and vertical components are shown in Figs. 8 to 10. The higher longitudinal turbulence intensity of the flow was observed in turbulent mixing layer near the obstacle top in the

wake region at $X/H = 0.125$, 0.375 , 0.625 and 1.125 due to large velocity gradient. While, the lower turbulence intensity is going upward, starting from the ground level, except near the obstacle top. The most features of the vertical and lateral turbulence intensity are the increase near the obstacle top and the slight deceleration at the upward direction.

3.1.4 Turbulent kinetic energy

The turbulent kinetic energy TKE was derived from the turbulent intensity in the longitudinal, lateral and vertical components, which measured along the centerline of the wind tunnel.

$$TKE = \frac{1}{2} \left(\overline{u^2 + v^2 + w^2} \right) \quad (4)$$

The turbulent kinetic energy is therefore greatly influenced in the entire flow field. Fig. 11 illustrates the turbulent kinetic energy around the obstacle wake region. The turbulent energy at $X/H = 0.125$, 0.375 , 0.625 and 1.125 gradually increased upwind from the ground surface and reached the maximum near the obstacle top and roughly constant for $1 < Z/H < 3$. This is due to an intense shear layer at the top of the obstacle model, where the kinetic energy of the mean flow is converted into turbulence kinetic energy (shear production of the turbulent kinetic energy). Moreover, the turbulent kinetic energy generated upwind of a given fixed point in the obstacle model will be exported downwind by local advection and turbulent transport.

3.3. The influence of obstacle on the dispersion characteristics

3.3.1. Mean concentration

The mean concentration characteristics were carried out through the neutral atmospheric conditions with the flow obstacle model at three downwind distances; $X/H = 0.375$, 0.625 and 1.125 , which are shown in Fig. 3. The vertical profiles of mean concentration were measured starting at 10 mm above the floor along the centerline of the wind tunnel, while the lateral profiles of mean concentration were measured at $Z/H = 0.5$. The mean concentration observed in this study was non-dimensionalized K by the reference velocity U_{ref} at obstacle height of 200 mm.

Figures 12 and 13 illustrate the vertical and lateral profiles of mean concentration at $X/H =$

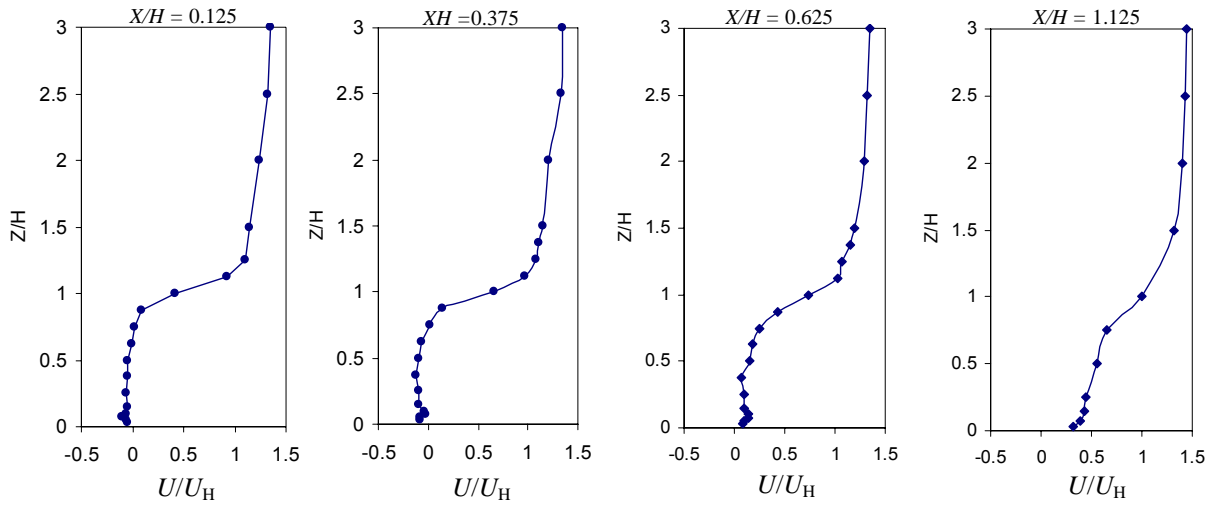


Fig. 5. Mean velocity component in the longitudinal direction (U/U_H)

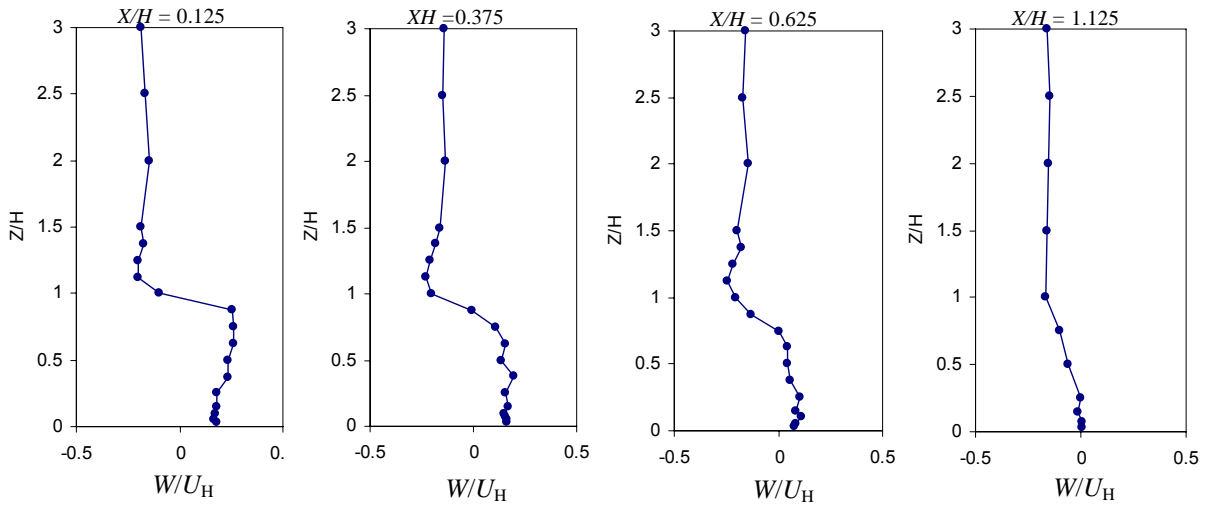


Fig. 6. Mean velocity component in the vertical direction (W/U_H)

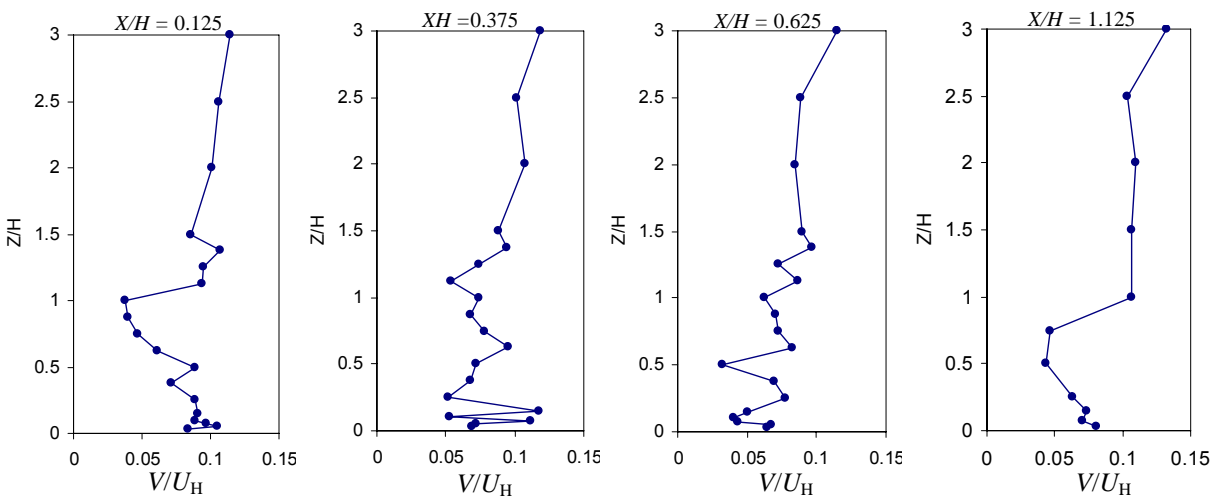


Fig. 7. Mean velocity component in the lateral direction (V/U_H)

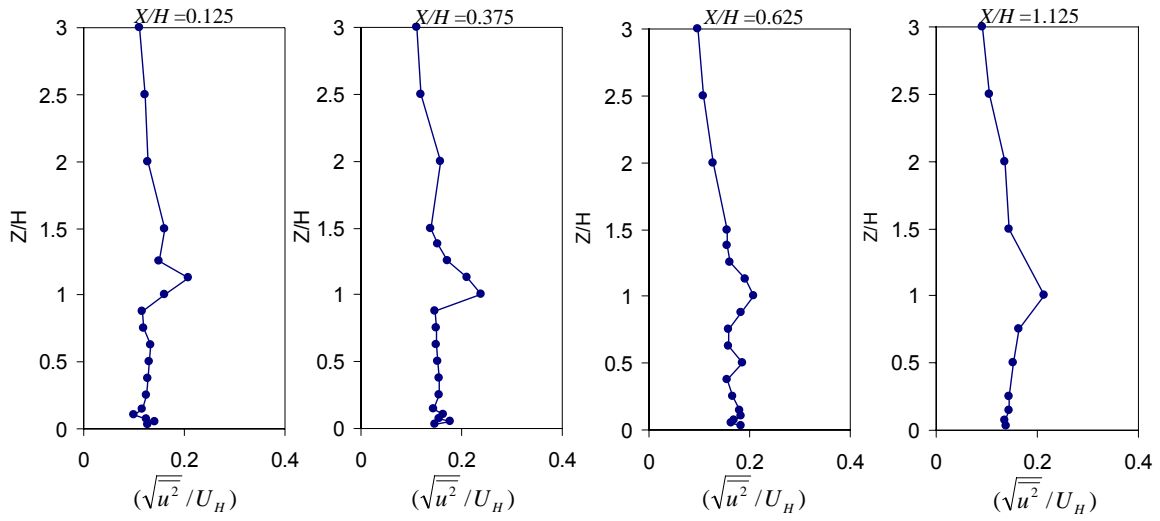


Fig. 8. Longitudinal turbulent intensity $(\sqrt{u^2}/U_H)$

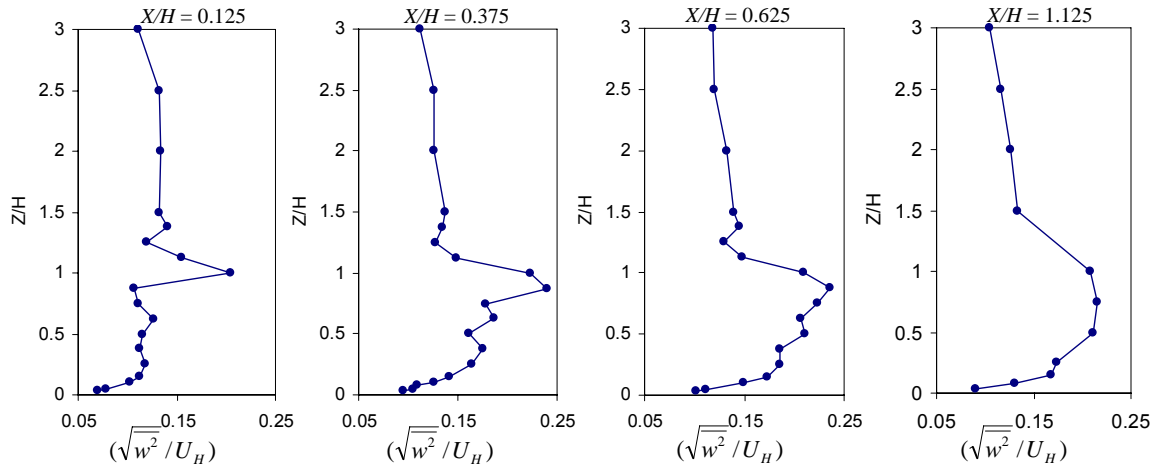


Fig. 9. Vertical Turbulent intensity $(\sqrt{w^2}/U_H)$

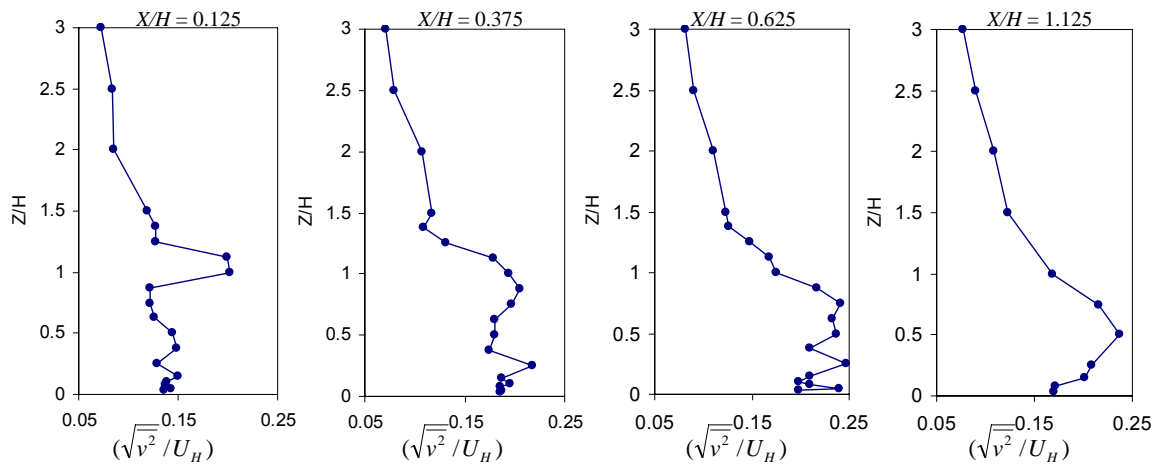


Fig. 10. Lateral Turbulent intensity $(\sqrt{v^2}/U_H)$

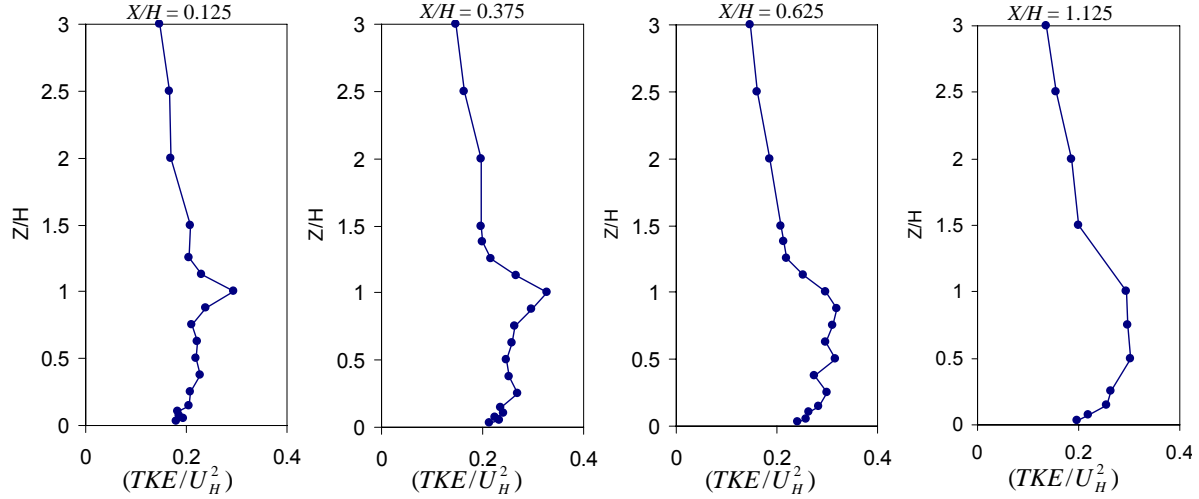


Fig. 11. Turbulent kinetic energy (TKE/U_H^2)

0.375, 0.625 and 1.125. The peak concentration was found 40 at $Z/H = 0.15$ respectively around the obstacle wake region at $X/H = 0.375$ near the gas source, where the effluent is emitted near the separation region and created the downwashes due to the emission velocity from the gas source was less than that of the free stream velocity. The lower mean concentration were observed at $Z/H = 1.25$ to 1.5 respectively due to the decreased turbulence intensity. The vertical mean concentration were gradually decreased upwind from the ground surface level and reached the minimum at $Z/H = 1.25$ respectively. The higher lateral mean concentration were found at $Y/H = 0$, while the lower lateral mean concentration were at both $Y/H = -0.25$ and 0.25 . The value of lateral mean concentration was not much different at $X/H = 0.625$ and 1.125 ; this is because these locations were far from the source gas. Therefore, these results indicate only a moderate effect on the change in concentrations due to the obstacle model. Close to the gas source, there is a noticeable effect of obstacle model on the mean concentration. Far from the gas source, the mean concentration was not much affected by the obstacle model. Thus, the smoothing of concentration differences was increased with downwind distance from the obstacle model.

3.3.2. Concentration fluctuation Intensity

The parameter most frequently used to characteristics concentration fluctuations is the fluctuation intensity, i

$$i = \sigma_x / C \quad (5)$$

$$\sigma_x = \left[\overline{(X_i - C)^2} / n \right]^{1/2} \quad (6)$$

where; σ_x is the concentration standard deviation, X_i denotes the instantaneous concentration and n is a series time. The concentration fluctuation intensity were non-dimensionalized i by the reference velocity U_{ref} at obstacle height of 200 mm.

Figures 14 and 15 displays the vertical and lateral profiles of the concentration fluctuation intensity at various downwind distances from the obstacle model; $X/H = 0.375, 0.625$ and 1.125 . The concentration fluctuations intensities were found to be less than 1 for all various locations. The higher concentration fluctuation intensity was appeared near the ground surface around the obstacle wake region at $X/H = 0.375$ than other heights. Furthermore, the vertical profile varies only slightly between $Z/H = 0$ to 0.25 , decreases rapidly to 0.375 and roughly constant for $0.375 < Z/H < 1$. The lower concentration fluctuations intensities were observed around the obstacle wake region at $X/H = 1.125$. The lateral profile of the concentration fluctuation intensity varies only slightly between $Y/H = -0.25$ to 0.25 , but the vertical profile varies small between $Z/H = 0$ to 0.9 . Despite similarities in the general shapes of the lateral and vertical profiles of fluctuation intensity to those observed in non-buoyant plume, the curves of i here are nevertheless wider and flatter, another manifestation of observed increase in the lateral and vertical plume spread.

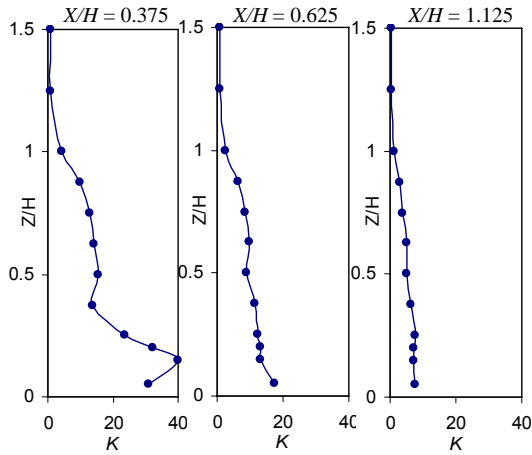


Fig. 12. Vertical profiles of mean concentration

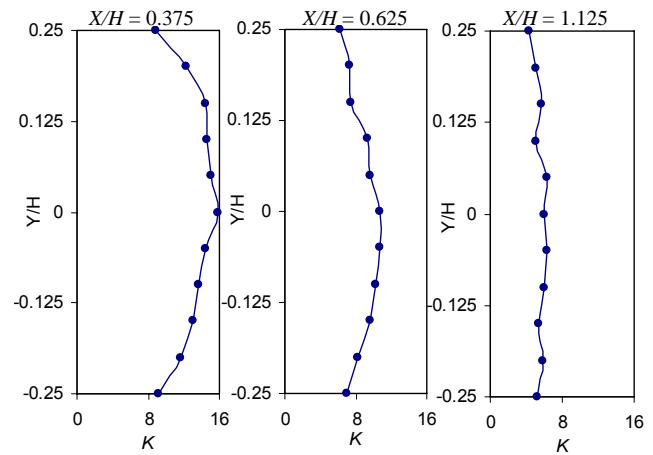


Fig. 13. Lateral profiles of mean concentration

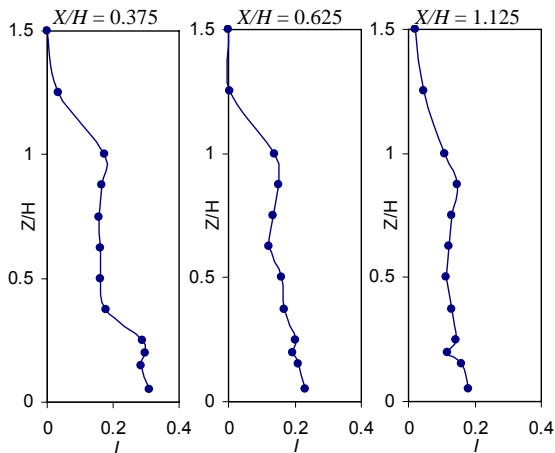


Fig. 14. Vertical profiles of concentration fluctuation intensity.

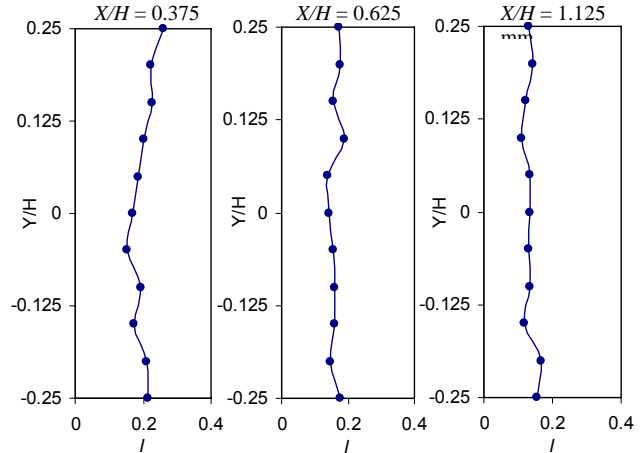


Fig. 15. Lateral profiles of concentration fluctuation intensity.

The obstacle model has effect of adding turbulence to the wake region, but at the scales smaller than the boundary layer scales. The scales are appreciably smaller close to the model than further downstream in the wake. If the variance of concentration can be treated as a transportable quantity, then it can be transferred and dissipated in the same way as turbulence kinetic energy (Wen-Whai et al., 1983). Therefore, the energy dissipation rates are higher in the obstacle wake than in the boundary layer, since they increase with decreasing turbulence length and time scales. Consequently, the fluctuation intensities observed in the near wake region dissipate faster than in the unobstructed boundary layer. This is reason why the lower fluctuations intensities were observed in the obstacle wake during the present work.

4. SUMMARY AND CONCLUSIONS

The effect of obstacle model on the flow and

pollutant dispersion in an urban environment using wind tunnel experiments under neutral atmospheric conditions may be summarized as the follows: (1) The vertical profiles of the longitudinal mean velocity are very thick around the obstacle wake region; (2) The longitudinal mean velocity was increased up near the obstacle top; (3) Inverse flows were observed up to a height of $X/H = 0.625$ around the obstacle wake region; (4) The longitudinal, vertical and lateral turbulence intensity were increased near the obstacle top; (5) The peak mean concentration was near the ground level around the obstacle wake region at $X/H = 0.375$; (6) The concentration fluctuations intensity were found lower near the obstacle top at $X/H = 1.125$; (7) The higher fluctuations intensity was observed near the ground surface around the obstacle wake region at $X/H = 0.375$ and; (8) The smoothing of concentration differences was increased with downwind distance from the obstacle model.

ACKNOWLEDGEMENTS

This work was carried out with funding from Japan Society for the Promotion of Science (JSPS).

REFERENCES

- Boerner, T., Leutheusser, H.J., 1984: Calibration of split fiber probe for use in bubbly two-phase flow. *DISA Info.*, 29, 10-13.
- Castro, I.P. and Snyder, W.H., 1982: A wind tunnel study of dispersion from sources downwind of three-dimensional hills. *Atmospheric Environment*, 16, 869-1887.
- Davidson, M.J., Mylne, K.R., Jones, .D., Phillips, J.C., Parkins, R.J., Fung, J. C. H. and Hunt, J. C. R., 1995: Plume dispersion through large groups of obstacles. *Atmospheric Environment*, 29, 3245-3256.
- Davidson, M. J., Snyder, W. H., Lawson, Jr. R.E. and Hunt, J. C. R., 1996: Wind tunnel simulations of plume dispersion through groups of obstacles. *Atmospheric Environment*, 30(22), 3715-3731.
- Higson, H.L., Griffiths, R.F., Jones, C.D. and Hall, D.J., 1994: Concentration measurement around an isolated building: A comparison between wind tunnel and field data. *Atmospheric Environment*, 28, 1827-1836.
- Hunt, J.C.R. and Mulhearn, P.J., 1973: Turbulent dispersion from sources near two-dimensional obstacles. *J. Fluid Mech.*, 61, 245-274.
- Kim, S., Brandt, H. and White, B.R., 1990: An experimental study of two dimensional atmospheric gas dispersion near two objects. *Boundary Layer Meteorology*, 52, 1-16.
- Kiya, M., Sasaki, K., 1983: Structure of turbulent separation bubble. *J. Fluid Mech.* 137, 83-113.
- Meroney, R. N., 1982: Turbulent diffusion near building. In Plate, E. (Ed), *Engineering Meteorology*, 481-525, Elsevier, Amsterdam
- Macdonald, R. W. and Griffiths, R. F., 1997: Field experimental of dispersion through regular arrays of cubic structures. *Atmospheric Environment*, 31(6), 783-795.
- Macdonald, R.W., Griffiths, R.F. and Hall, D.J., 1998: A comparison of results from scaled field and wind tunnel modeling of dispersion in arrays of obstacles. *Atmospheric Environment*, 32, (22), 3845-3862.
- Mavroidis, I., Griffiths, R. F., Jones C.D. and Bilotta C.A., 1999: Experimental investigation of the residence of contaminants in the wake of an obstacle under different stability conditions. *Atmospheric Environment*, 33,939-949.
- Mavroidis, I. and Griffiths, R.F., 2001: Local characteristics of atmospheric dispersion within building arrays. *Atmospheric Environment*, 35, 2941-2954.
- Mavroidis, I., Griffiths, R.F. and Hall, D.J., 2003: Field and wind tunnel investigations of plume dispersion around single surface obstacles. *Atmospheric Environment*, 37, 2903-2918.
- Mfula, A.M., Kukadia, V., Griffiths, R.F. and Hall, D.J., 2005: Wind tunnel modeling of urban building exposure to outdoor pollution.
- Snyder, W.H., 1981: Guideline for fluid modeling of atmospheric diffusion. EPA -600/8-81-009. *Atmospheric Environment*, 39, 2737-2745.
- Wen-Whai, L. and Meroney, R.N., 1983: Gas dispersion near a cubical model building: Part II: Concentration fluctuation measurements. *J. Wind Eng. and Industrial Aerodyn.*, 12, 35-47.